Numerical Study on Influential Factors Affecting Drag Reduction Effect of Bionic Microscopic Riblets Surface

Chao XU, Jing WANG*, Bing QU，Lanyu JIANG
School of Science, Dalian Ocean University, China
*Corresponding author. E-mail: wangj@dlou.edu.cn

Abstract

The bionic non-smooth riblets surface which based on the study of shark skin scales' microscopic structure provides a new kind of low-drag surface microscopic topological structure. In this paper, the possible influential factors to the drag reduction effect of bionic microscopic riblets structure are proposed through the fluid numerical simulation and analyses. The drag reduction effect of riblets structure depends on the coactions of fluid velocity inlet, riblets' size and apex angle. The study provides some new ideas to design better surface with micro riblets structure and supported to explore proper flow field conditions to use riblets technique.

Keywords: bionic non-smooth technology; drag reduction; microscopic riblets; computational fluid dynamics(CFD)

1 Introduction

The oceanic nektons are able to interact with water effectively and the interactions can reduce the resistance and save their energy when moving forward. The drag reduction effect of the riblets which based on the bionic study of shark skin has attracted extensive attentions worldwide. The rib-like bionic non-smooth surface provides a new kind of low-drag surface microscopic topological structure for the structural design of ships and varieties of oceanic vehicles[1].

The riblets technology can be widely used and has huge potential for growth according to its satisfactory reliability and applicability. It has been put into trial applications in the field including surfaces of watercraft and aerocraft, inner wall of pipeline and athletic swimsuit[2]. Additionally, some of the correlational researches have forecasted and reported the drag reduction rate of the riblets. Reports claimed that bionic riblets with specific shape could have a drag reduction rate over 30%[3]. The Coustols' experiment got the drag reduction rate of 10~15%[4]. Walsh gained the drag reduction rate up to 8%[5].

The riblets technology as a pollution-free drag reduction scheme has important meaning to the coordinated and sustainable development of ship and marine industry.

Though the research of riblets technology in and abroad made certain progress, many questions remain unanswered. Especially the influential factors affecting drag reduction effect of the riblets surface remain unclear. The fluid numerical experiment of the paper aimed to analyze and discuss the possible influential factors and to provide theoretical support for correlational studies.

2 Model Design and Numerical Method

2.1 The Prototypes of Microscopic Riblets Surface

Rib-like scales of the *squalus brevirostris*' skin shown in Fig.1 was observed by SEM. The *squalus brevirostris* was bought in the fish market of Dalian City and the scales were well sampled. In the figure, the scales were made up of parallel riblets which were almost parallel to lateral line of the shark (arranged in flow direction) and the riblets of adjacent scales correspond to each other.

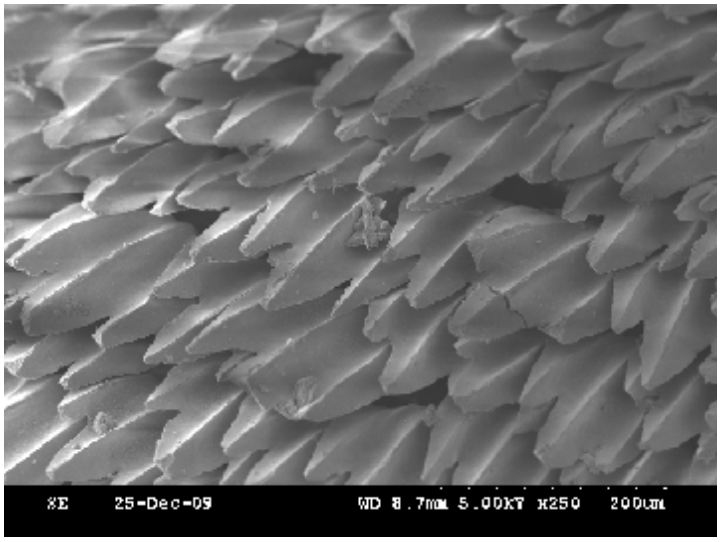

Fig.1 Rib-like scales of the *squalus brevirostris*' skin

2.2 Experimental Model Design

A section of spacial domain was chosen to calculate (Fig.2). The bottom surface of the domain was set as a downstream riblets surface while the top surface was set as a flat surface which had the same roughness coefficient to the bottom one. Constructed the flat and the riblets surface in a same flow field could not only avoid too many computational costs, but also reduce the capacity calculation error when simulating the flat surface separately. The height of spacial domain was 2×10^3μm which could keep the flat surface unaffected by the upward flow caused by the riblets' tip. The length of the domain was 4×10^3μm. Eight continuous riblets were laid up along the flow direction.

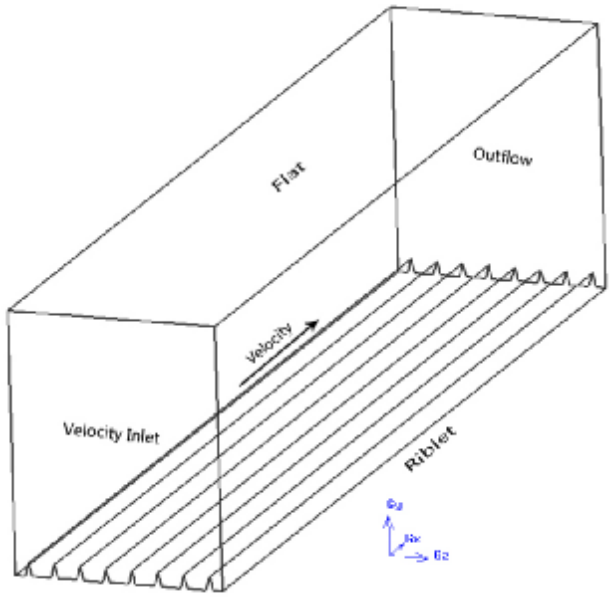

Fig.2 The three-dimensional computational domain

Six models with two different sizes and shapes were introduced to calculate and compare the drag reduction rate at different conditions. The parameters of the six models were listed in Tab.1. The "*s*", "*h*", "*α*" respectively represented the distance between two ridges, the height and the apex angle of riblets.

Tab.1 Parameters of the six models

Model Identifiers	***s*** **(μm)**	***h*** **(μm)**	***α*** **(°)**	**Shape Sketches of riblets**
1	100	50	30	
2	100	50	60	
3	100	50	90	
4	60	30	30	
5	60	30	60	
6	60	30	90	

2.3 Model Discretization

Considered the calculation accuracy and the computational cost, the model was discretized in some particular methods. Due to the tiny size of the model, grid size of flat and riblets surface should be small enough to fully reflect the turbulent boundary flow. Both velocity inlet and outlet surface were discretized by triangular unstructured meshes. The instability of the meshes with different magnitudes and types could be effectively prevented by using the unstructured meshes. According to reference [5],

ratio could be set to adjust the grid distribution due to the special shaped riblets structure. After the meshing, the grids in adjacent area of flat and riblets surface were dense while the rest were sparse. Besides, set the inlet and outlet surface as periodic boundary condition in order to make the two surfaces have a same distribution of grid nodes. The fluid domain along the flow direction was discretized by hexahedral grids. The meshes of the model were shown in Fig.3.

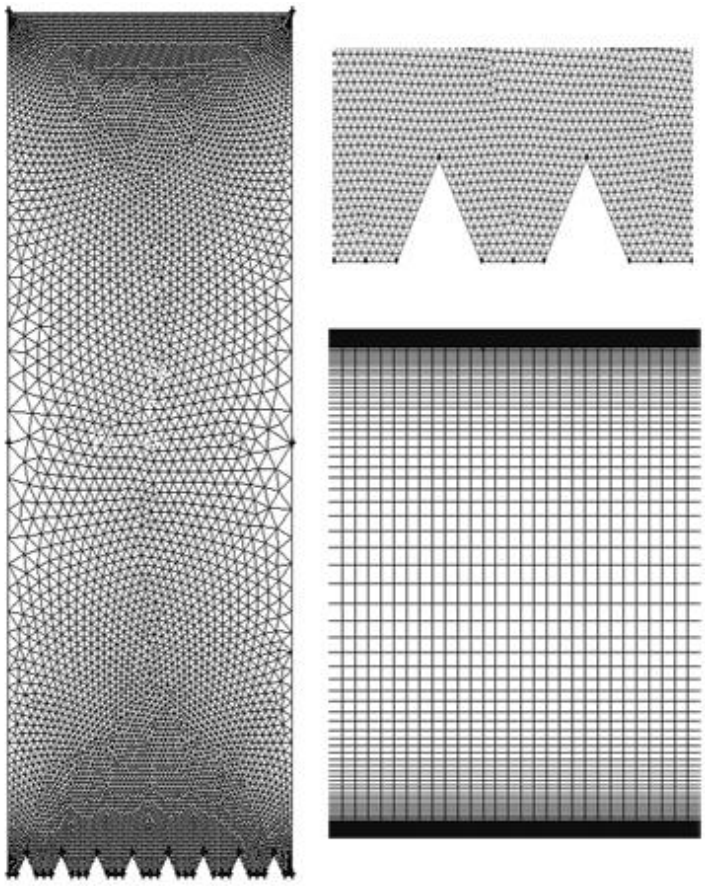

Fig.3 Meshes of the model

2.4 Specify Boundary Types

Fluid inlet surface: velocity inlet.

Fluid outlet surface: outflow.

Flat and riblets surface: stationary wall (no slip).

Left and right borders: symmetry.

2.5 Numerical Parameters

Fluid properties: $\rho=1.025\times10^{3}\mathrm{kg/m^{3}}$, $\upsilon=1.1883\times10^{-6}\mathrm{m^{2}/s}$.

Flow velocity: 6m/s.

Discretization schemes: second order upwind.

Solver: segregated.

Pressure-velocity coupling: SIMPLE algorithm.

Viscous model: RNG k-ε (2 eqn) model.

Near-wall treatment: enhanced wall treatment.

2.6 Computational Formula of Drag Reduction Rate

Viscous friction coefficient formulas of flat and riblets surface were listed as follows.

$$C_{f\text{-flat}} = F_{f\text{-flat}}/(1/2\rho u^2 S_{\text{flat}}) \quad (1)$$

$$C_{f\text{-riblets}} = F_{f\text{-riblets}}/(1/2\rho u^2 S_{\text{flat}}) \quad (2)$$

In the above formulas, "C_f" represented surface viscous friction coefficient, "F_f" represented the viscous friction, "u" represented the fluid velocity, "S" represented wetted surface area, subscript "flat" meant the flat surface while the subscript "riblets" meant the riblets surface.

The riblets drag reduction rate η relative to flat surface could be counted as the following formula.

$$\eta = [(C_{f\text{-riblets}} - C_{f\text{-flat}})/C_{f\text{-flat}}] \times 100\% \quad (3)$$

If η was calculated as a positive value, the resistance of riblets was greater than that of flat surface. The situation was opposite when the value of η was negative.

3 Results

The experiment calculated different types of riblets structure at different fluid velocity conditions and the viscous friction coefficients of flat and riblets surface were gained. Thus the maximum drag reduction rate of riblets relative to flat was gained.

3.1 Analysis of the experiment accuracy

In order to test and verify whether the numerical method was effective and accurate, in comparison with previous documentary results was necessary. The comparison results of viscous friction coefficient of flat surface with same Reynolds number to the previous experiments were shown in Tab.2.

Tab.2 Comparison results of viscous friction coefficient

Reynolds Number	$C_f \times 10^3$		
	Result of the simulation	Result of Dean's experiment	Result of Moser's experiment
10935	0.0056	0.0061	0.0059

From the Tab.2, the error between our experiment and Dean's[6] experiment was 8.19% while the error between our experiment and Moser's[7] experiment was 5.08%.

The comparison results indicated that the numerical method of our experiment was reliable.

3.2 Fluid velocity's impact on drag reduction

The drag reduction rate and its variation with different fluid velocity inlet were obtained as Fig.4.

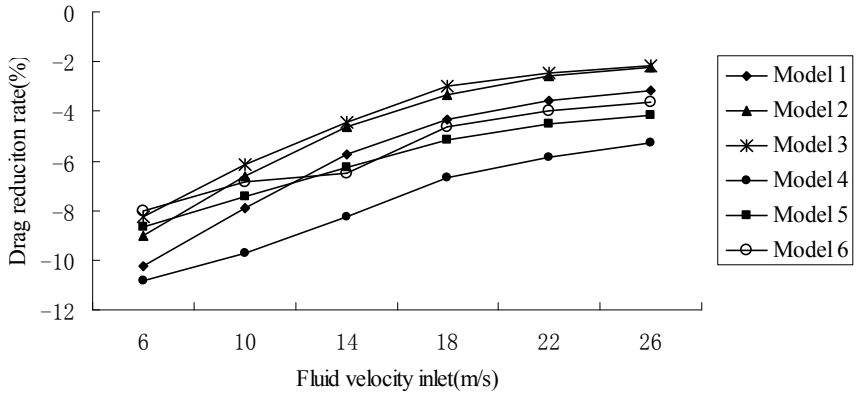

Fig.4 Relationship between drag reduction rate and velocity inlet of each model

As shown in Fig.4, all six riblets models demonstrated superior drag reduction effect and showed almost the same trends. The maximum drag reduction rate turned up when the fluid velocity inlet was 6m/s which indicated that riblets structure had better effectiveness in low fluid velocity range. The maximum drag reduction rate of six models were 10.23%, 9.01%, 8.23%, 10.81%, 8.67%, 8.04%. From the curvilinear trend we could also predict that with the increasing of fluid velocity the drag reduction effect of riblets structure would approach zero or even increase the drag especially for the riblets models with larger apex angles.

3.3 Riblets size's impact on drag reduction

The drag reduction rate distributions with different riblets sizes were obtained as Fig.5.

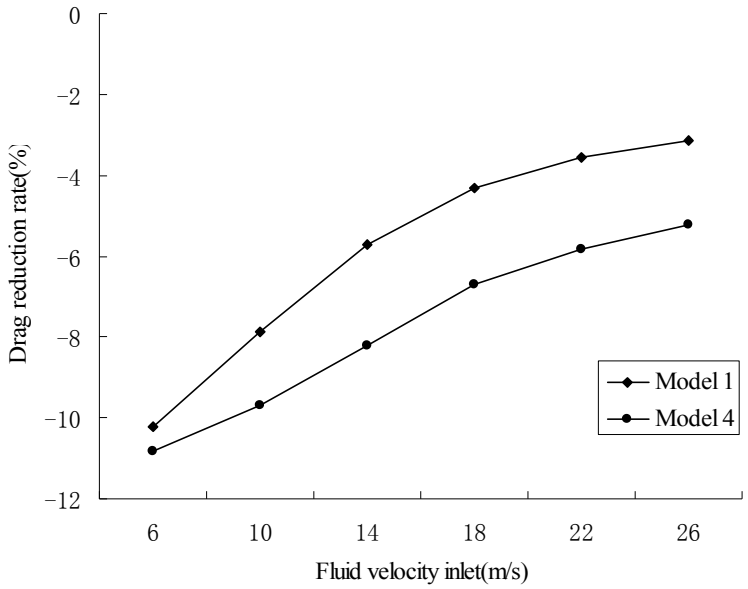
0
−2
−4
−6
−8
−10
−12
Drag reduction rate(%)
6
10
14
18
22
26
Fluid velocity inlet(m/s)
Model 1
Model 4

(a)

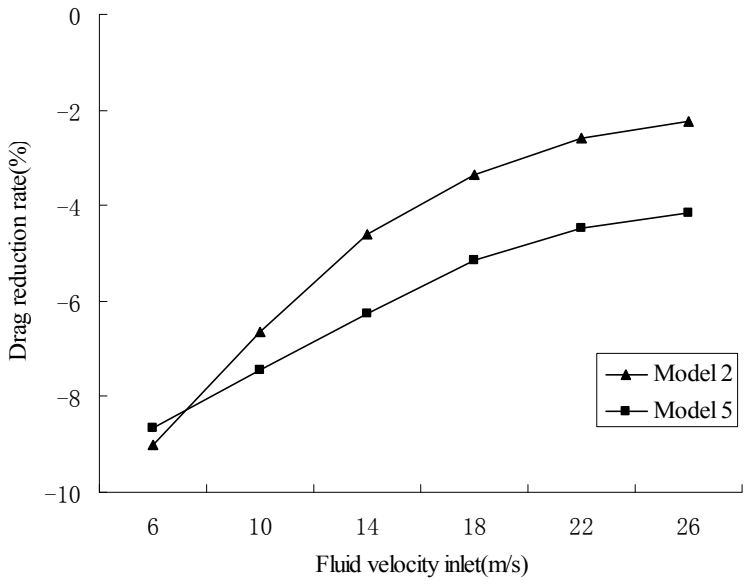
0
−2
−4
−6
−8
−10
Drag reduction rate(%)
6
10
14
18
22
26
Fluid velocity inlet(m/s)
Model 2
Model 5

(b)

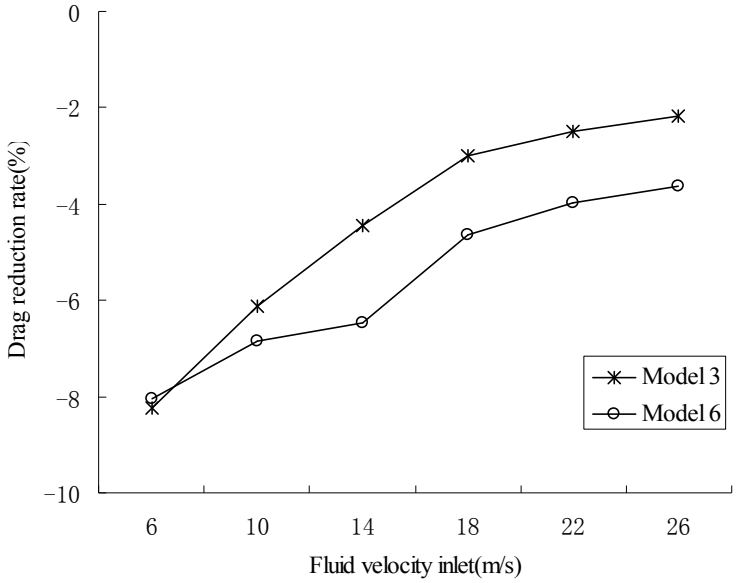

(c)

Fig.5 Relationship between drag reduction rate and sizes of riblets

(a) α=30° (b) α=60° (c) α=90°

As shown in Fig.5, though the drag reduction effects of the models with different sizes demonstrated the same trend, there were certain gaps. By comprehensive comparison in general fluid velocity ranges, the riblets structure with smaller sizes had better drag reduction effect.

3.4 Ridge shape's impact on drag reduction

The drag reduction rate distributions with different riblets apex angles were obtained as Fig.6.

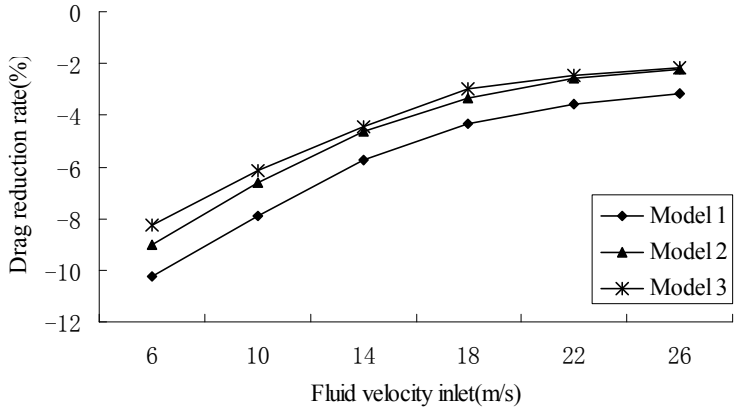

(a)

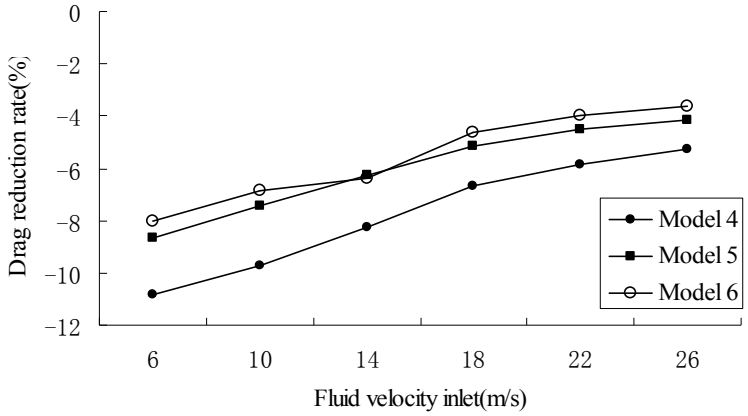

(b)

Fig.6 Relationship between drag reduction rate and apex angles of riblets

(a) s=100μm, h=50μm (b) s=60μm, h=30μm

From Fig.6, the drag reduction rates of the models turned to be obviously different when they had the same sizes but different apex angles. The maximum drag reduction happened in the riblets models with 30° angle in both figure 6(a) and 6(b). We could draw a conclusion from the curvilinear trends that the drag reduction rate of riblets structure would gradually decrease with the increasing of riblets apex angle.

4 Conclusion

The RNG k-ε viscous model is suitable for the high strain rate and full developed turbulent flow in the experiment. This method can obtain successful results in the model with a high Reynolds number.

Through the fluid numerical simulation and analyses, the possible influential factors to the drag reduction effect of bionic microscopic riblets structure are proposed. The drag reduction effect of riblets structure depends on the coactions of fluid velocity inlet, riblets' size and apex angle. Any change of the three factors will make the drag reduction effect change. The conclusion provides some new ideas to design better surface with micro riblets structure and support to explore proper flow field conditions to use riblets technique.

References

[1] Chao Xu, Jing Wang, Shuguang Luan, Bing Qu, Lanyu Jiang: Analysis of drag reduction mechanism of the bionic microscopic riblets surface, *2010 3rd International Conference on Biomedical Engineering and Informatics*, 2010, 2394-2398.

[2] Xu Chao, WANG Jing, LIU Ya-chen, JIANG Lan-yu: A review: the research and

application of drag reduction by biomimetics riblets technique, *Journal of Dalian Fisheries University*, **24**(2009), 235-237.

[3] WU Ming-kang: Application and development of the imitation shark skin swimsuits, *Progress in Textile Science & Technology*, **2**(2009), 90-91.

[4] Coustols E: Behavior of internal manipulators: 'Riblet' models in subsonic and transonic flows, *AIAA*, 1989, 89-0963.

[5] Walsh M. J: Turbulent boundary layer drag reduction using riblets, *American: AIAA*, 1982.

[5] HU Hai-bao, SONG Bao-wei, DU Xiao-xu, MA Ji: Research on numerical computation of near-wall fluid field on grooved surface, *Fire Control and Command Control*, **33**(2008), 54-56.

[6] Dean R B: Reynolds Number Dependence of Skin Friction and Other Bulk Flow Variables in Two-dimensional Rectangular Duct Flow, *J. Fluids Eng*, **100**(1978), 215-223.

[7] Moser R D, Kim J, Mansour N N: Direct numerical simulation of turbulent channel flow up to Re=590, *Phys. Fluids*, **11**(1999), 943-945.

Acknowledgement

Project "Biomimetic research of materials with tailored surface micro- and nano-architecture for prevention of marine biofouling" supported by the National Natural Science Foundation of China (50773010).

Received July 27, 2010
Accepted November 25, 2010